PAPER

Check for updates

Comparison of the efficacy of seven types of microneedles for treating a rabbit hypertrophic scar model†

Fang Liu,‡[a] Yingzhi Luo,‡[b] Huan Chen,[a] Shengjing Xu,[c] Dongyan Zhang,[c] Hong Sang,*[a] Chenjie Xu [iD] *[d] and Min Zhang*[c]

Microneedle technology can effectively suppress the formation of hypertrophic scarring in both animals and humans. Our previous research has revealed that this is due to the physical contact inhibition effect by using microneedles made of liquid-crystal polymers as the model device. One important factor we didn't study is the influence of the fabrication materials of microneedles. Therefore, this article examines this key point on a rabbit ear hypertrophic scar model. We monitor the thickness of the scars, and the expression of α-SMA and Ki-67 protein, and TGF-β1 mRNA in a period of 42 days. Among microneedles made of 6 polymeric materials and stainless steel, polymethylmethacrylate microneedles present superiority in all aspects including the reduction of tissue fibrosis, and the expression of α-SMA, Ki-67 protein and TGF-β1 mRNA. On the other hand, polycarbonates, polyurethane, and polylactic-*co*-glycolic acid microneedles could suppress three biomarker expressions.

1 Introduction

Abnormal scars including hypertrophic scars and keloids can be aesthetically displeasing and lead to severe psychological impairment. Wound healing, as well as the process of scarring, is an essential course for repairing common damage caused by physical trauma, surgical incisions and other unexpected injuries.[1–3] To date, though an abundance of novel therapies and technologies such as the aesthetic stitching technique, and new dressing biomaterials[4,5] have been applied for the improvement of the process, the number of patients suffering from scarring problems is continuing to increase. It is estimated that there are more than 100 million new scar patients every year worldwide, and about 20% of them are affected by abnormal scars. Similarly, despite the fact that many invasive and non-invasive options are available for patients to treat scars, their efficacy is unsatisfactory, and these interventions are often accompanied by multiple side-effects.[6–11]

Previously, our team reported the usage of microneedle (MN) arrays made of liquid-crystal polymers (LCP) to treat keloid and hypertrophic scars.[12] These MNs with the length of 500–1000 μm reach the dermis layer without causing pain and infection. Interestingly, drug-free MNs inhibited the proliferation of skin fibroblasts and thus reduced scar growth (contact inhibition effect) in both animals and patients.[13,14] Medicine can also be embedded in the polymeric matrix of MNs to further improve the anti-scar effects.[15,16]

In fact, the mechanism of scar formation is complicated. Briefly, multiple inflammatory cells are activated in the process of wound healing and plenty of cytokines particularly transforming growth factor β (TGF-β) are synthesized and released, driving the fibroblast proliferation and development of alpha-smooth muscle actin (α-SMA)$^+$ myofibroblasts from fibrocytes and proto-myofibroblasts.[2,17,18] Myofibroblasts play a central role in the dysregulated and excessive production of collagen-rich extracellular matrix, the scars. As reported, the effect of microneedle arrays in the treatment of scars is due to physical contact that inhibits fibroblast viability. Therefore, self-administrated, minimally invasive drug-free MNs provide an application prospect to scar patients. However, one key factor we didn't study is the influence of materials on the anti-scarring effect of MNs, because each material has its unique chemical and physical properties. Meanwhile, it is essential to find a cost-effective material for the practical application of MNs. Therefore, this work (Fig. 1) looks into the anti-scarring effect of MNs made of seven biomaterials including LCP, polycarbonates (PC), polyurethane (PU), polylactic-*co*-glycolic acid (PLGA), poly-methylmethacrylate (PMMA), polypropylene (PP), and stainless

[a]Department of Dermatology, Jinling Hospital, School of Medicine, Nanjing University, Nanjing, China. E-mail: sanghong@nju.edu.cn

[b]Department of Dermatology, Affiliated Hangzhou First People's Hospital, Zhejiang University School of Medicine, Hangzhou 310006, China

[c]Department of Dermatology, The Affiliated Jiangning Hospital with Nanjing Medical University, Nanjing 211100, China. E-mail: zhangmin76ch@163.com

[d]Department of Biomedical Engineering, City University of Hong Kong, 83 Tat Chee Avenue, Kowloon, Hong Kong SAR, China. E-mail: chenjie.xu@cityu.edu.hk

† Electronic supplementary information (ESI) available. See DOI: https://doi.org/10.1039/d2na00604a
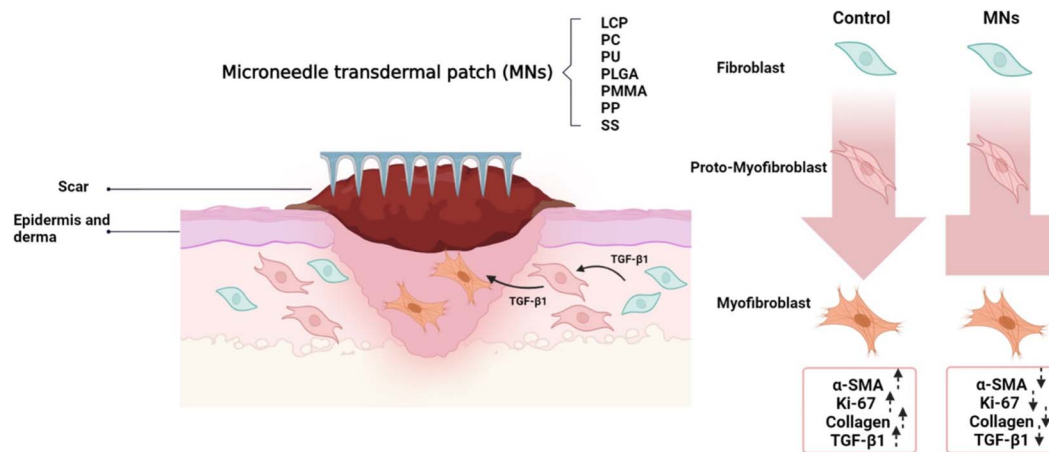
‡ These authors contributed equally to this work.

Fig. 1 Schematic illustration of MN treatment of a hypertrophic scar. The key scar biomarkers including collagen deposition, α-SMA and Ki-67 protein expression, and TGF-β1 mRNA expression were used to evaluate the efficacy of seven types of MNs for hypertrophic scars. Note: LCP: liquid-crystal polymers, PC: polycarbonates, PU: polyurethane, PLGA: polylactic-*co*-glycolic acid, PMMA: polymethylmethacrylate, PP: poly-propylene, SS: stainless steel.

steel (SS). On the rabbit ear hypertrophic scar model, we monitor the thickness of the scars, tissue fibrosis, and the expression of α-SMA (a marker of fibroblasts) and Ki-67 protein (a marker of proliferation), and TGF-β1 mRNA in a period of 42 days.

2 Methods

The main reagents of anti-α-SMA (ab7817) and anti-Ki-67 (ab15580) antibodies were ordered from Abcam. Horseradish enzyme-labeled goat anti-rabbit IgG (H + L) (ZB-2301) and anti-mouse IgG (H + L) (ZB-2305) were purchased from Golden Bridge. Hematoxylin staining (AR1180-1) and Picro-Sirius Red Staining Solution (G1470) were ordered from Bosond Bio and Solvay, respectively. The commercial kits of DAB (3,3-*N*-di-aminobenzidine tertrahydrochloride) color development kit (CW0125), Ultrapure RNA Extraction Kit (CW0581M), HiFiScript cDNA First-Strand Synthesis (CW2569M) and UltraSYBR Mixture (CW0957M) were ordered from CWBIO Kang Century. Female Japanese big ear rabbits (age 8–10 weeks, weight 1.5–2.5 kg) were ordered from Nanchang Longping Rabbit Industry Co., Ltd. All animal procedures were performed with the Guidelines for Care and Use of Laboratory Animals of Nanjing University and approved by the Animal Ethics Committee of Jinling Hospital (B2019-73).

2.1 MN patch

Polymeric MNs were purchased from Micropoint Technologies Pte Ltd (Singapore). They are MNs of LCP, PC, PU, PLGA, PMMA, PP, or SS (Fig. 2). All MN tips shaped as pyramids have a height of 500 μm and were arranged on the patch (a 10×10 needle array) with a density of 21 needles per cm^2 as in a previous study.[13]

2.2 Setup of the rabbit ear hypertrophic scar model

The scar model was built similarly as a previous report[10] (Fig. 3). Rabbits were anesthetized by intraperitoneal injection with ketamine (60 mg kg^{-1}) and xylazine (5 mg kg^{-1}) before the surgery. Then, the round skin with a diameter of 1 cm from the periosteum of the rabbit ear was removed from the ventral surface using a skin biopsy ring. The wound was hemostatic and exposed, and the cartilage was scraped off. Four round wounds were established and separated by more than 15 mm on each rabbit ear (Fig. 3a). Each rabbit was fed in a single cage under the same condition with food and water access. The fresh wound crust was removed 1 week later (Fig. 3b), and when the new crust fell off spontaneously after 20 days (Fig. 3d), the hypertrophic scar model was established.

2.3 MN treatment of hypertrophic scars in the rabbit model

Hypertrophic scars were established on both ears of 24 rabbits. The scars of all right ears were randomly treated with LCP, PC, PU, PLGA, PMMA, PP or SS MNs. The device was placed over the hypertrophic scar and fixed with translucent 3M Tegaderm® tape. The medical tape without MNs applied to the right ear scars was set as the blank. Meanwhile, scars on the left ears were left to heal naturally. The thickness of the scar was measured weekly and calculated by subtracting the thickness of normal ear tissue from the thickness of the scar tissue. Meanwhile, rabbits were anesthetized and sacrificed on days 0, 21, and 42 of the treatment for histology analysis.

2.4 Picro-Sirius Red staining

Picro-Sirius Red staining was used to visualize the collagen I and III fibers in the scar tissues. Briefly, the scar tissues were fixed with 10% formalin solutions soon after sacrificing. The samples were dehydrated and embedded in paraffin. Subsequently, the paraffin section of each scar was dewaxed and
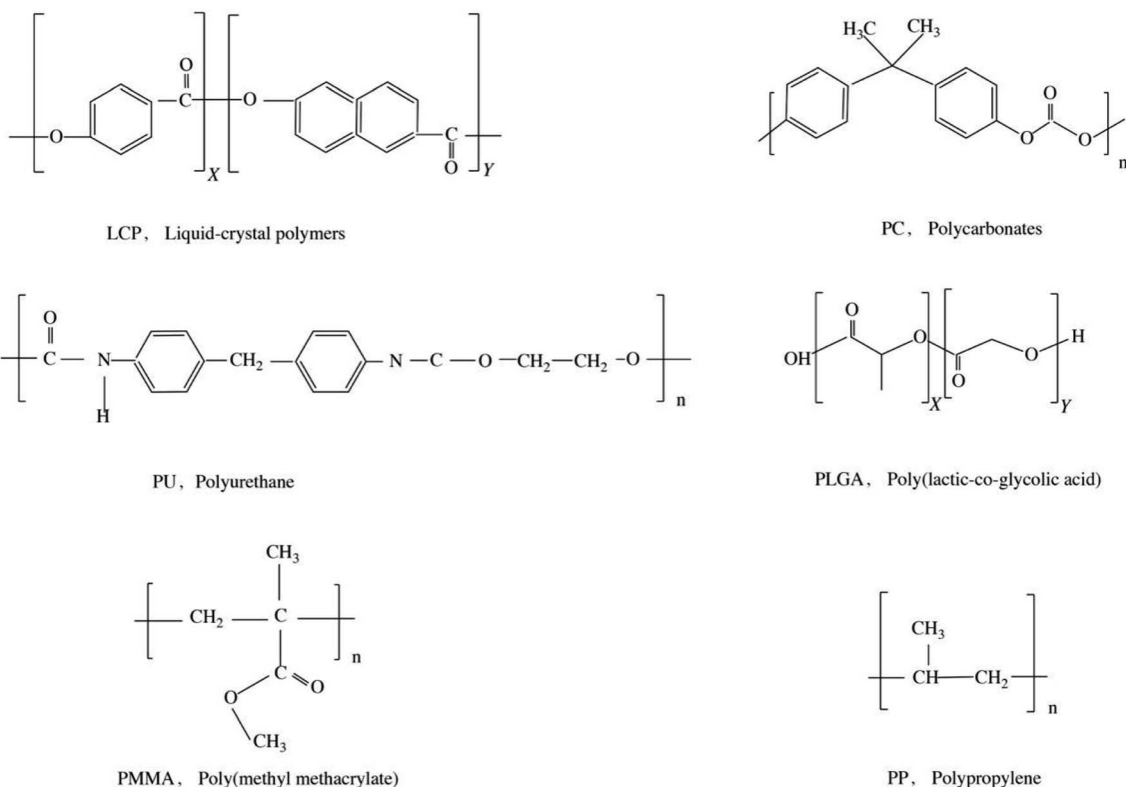
Fig. 2   The molecular formulas of 6 polymer materials for MNs.

hydrated. The sections were stained with Picro-Sirius Red according to the instruction of staining kits. A gradient concentration of ethanol was used for dehydration and xylene for vitrification. Finally, sections were sealed with neutral gum.

2.5   Immunostaining for Ki-67 and α-SMA protein

Paraffin sections of the scar tissues were baked, dewaxed and hydrated. The sections were placed in a repair box with antigen repair solution, and then heated for antigen recovery. Later the sections were transferred into a wet box and incubated with freshly prepared 3% hydrogen peroxide at room temperature for 10 min. After washing 3 times using phosphate buffer saline (PBS), the slides were blocked using 5% bovine serum albumin (BSA) at 37 °C for 30 min. Primary antibody was then added and incubated at 4 °C overnight. Secondary antibody solution (1 : 100) was added the next day and incubated at 37 °C for 30 min. Afterwards, fresh DAB solution was added and incubated for 5–10 min and then counterstaining was performed with hematoxylin. Sections were dehydrated with the gradient concentrations of alcohol and cleared with xylene. Finally, the slides were mounted with a coverslip for imaging.
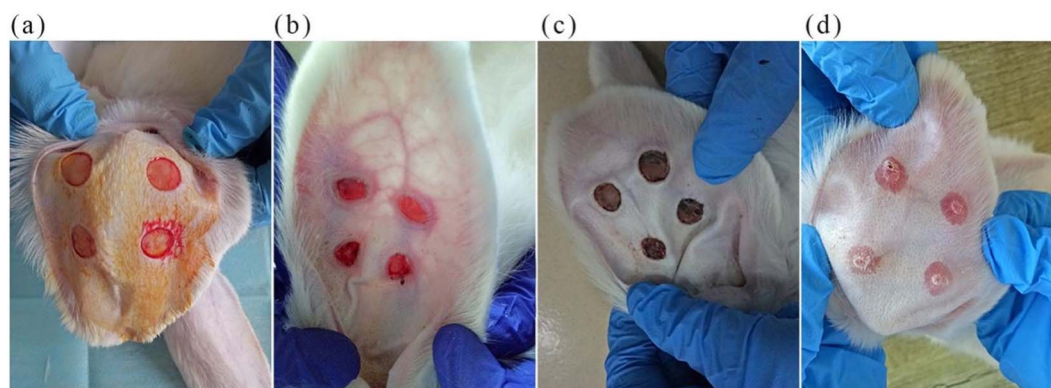

Fig. 3   The establishment of rabbit ear hypertrophic scar models: (a) four round wounds with a diameter of 1 cm were established and separated by more than 15 mm on each rabbit ear, day 0. (b) The fresh wound crust was removed on day 7. (c) The black crust was formed at day 14. (d) The new crust fell off spontaneously after day 20.
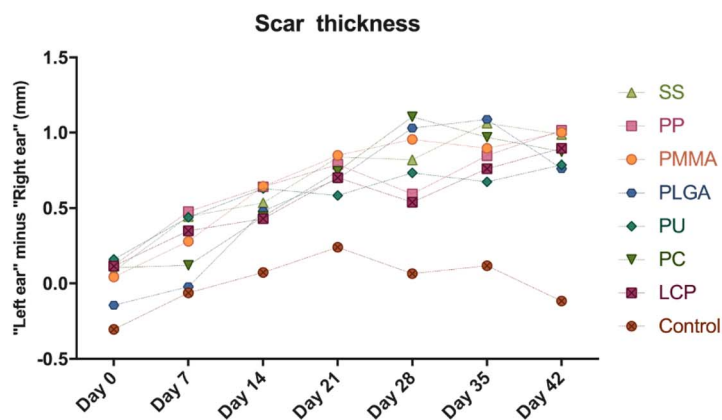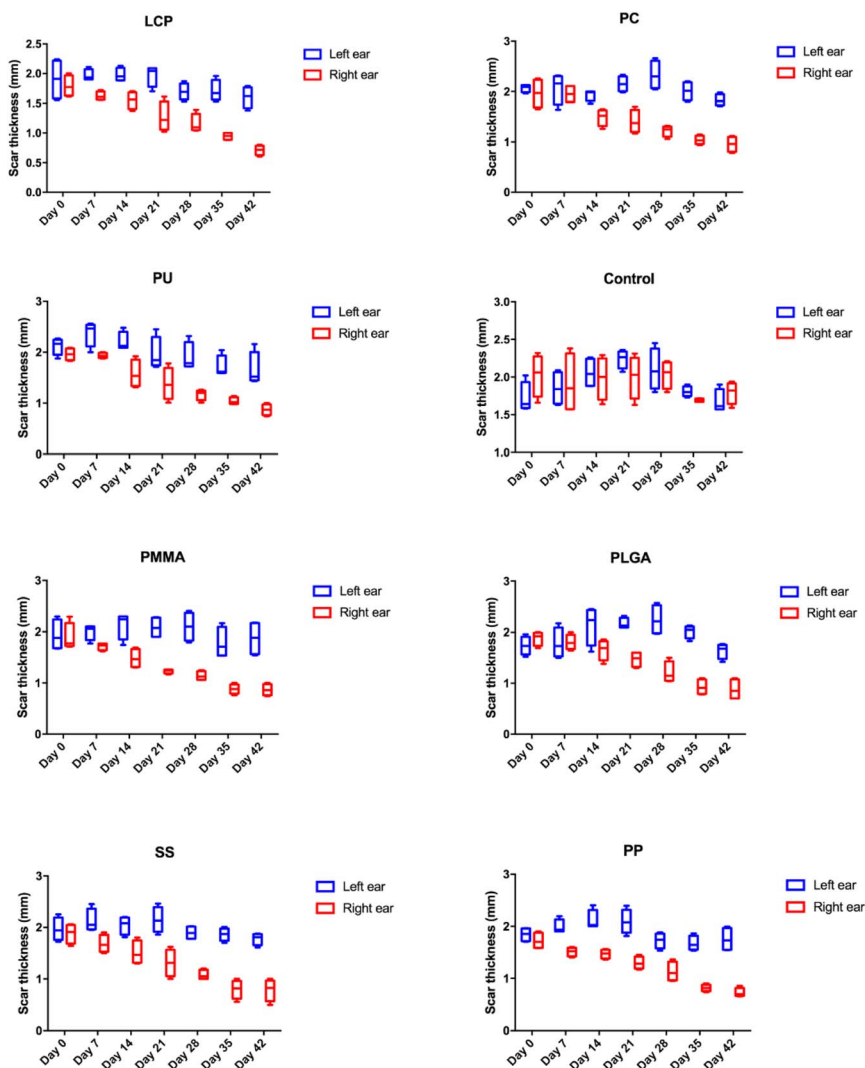
Fig. 4 The quantification of scar thickness during the MN treatment. (Top) The thickness of the scars on the MN treated ears was significantly reduced as time prolonged. (Bottom) The reduction showed no significant difference between each MN treated group ($P > 0.05$).

2.6 Quantitative analysis of scar tissue sections

Software Image J was used to conduct the measurement of the average optical density (AOD) of each scar section to evaluate the magnitude of the stain. Pictures were firstly transformed into an 8-bit form, and then calibration was performed from a grey value to optical density. Then the AOD of the targeted staining area can be highlighted and measured using the software automatically. Afterwards, the AOD ratio of the targeted staining area such as dermis for Picro-Sirius Red staining to stratum corneum was adopted to exclude the systematic error about the process of staining.

2.7 Real-time reverse transcriptase polymerase chain reaction (qRT-PCR)

Total RNA was extracted from the tissue sample in each group and then reverse transcribed into cDNA as a template. qRT-PCR was performed to detect TGF-β1. β-Actin was used as an internal control. Primer pairs are: TGF-β1 F CTGTACCAGAAATA-CAGCAACGAT, TGF-β1 R AGCCACTGCCTCACAACTCC, β-actin F CTGAACCCTAAGGCCAACCG, β-actin R GTCACGCACGATTT CCCTCTC.

2.8 Statistical analysis

All data are expressed as mean ± standard deviation (SD) analyzed using SPSS 19.0. The differences among the groups were evaluated by two-way analysis of variance (ANOVA) followed by the Tukey–Kramer multiple comparison test for more than two groups. The analysis was performed using GraphPad Prism 7 software (GraphPad Software Inc., USA). The difference was considered significant when $P < 0.05$ versus control group described in the legends.

3 Results

3.1 The rabbit ear hypertrophic scar thickness evaluation

The right ear scar showed good response after MN treatment and the thickness change of the scar is presented in Fig. 4. There is a significant reduction of the scar thickness on the right ear scar after the treatment of MNs when compared to that of the left ear
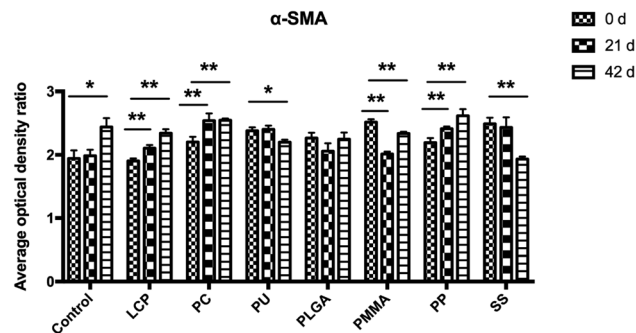

Fig. 6 The average optical density (AOD) ratio of α-SMA staining evaluated using software Image J at different time points. The expressions of α-SMA in PU, PLGA, PMMA, and SS groups were significantly decreased after MN treatments on day 42. *$p < 0.05$ and **$p < 0.001$ vs. 0 days ($n = 3$).

scar ($P < 0.05$). We also observe that this reduction became more significant as time went by in each MN treated group (top part of Fig. 4). However, the reduction showed no significant difference between each MN treated group ($P > 0.05$) (bottom part of Fig. 4).

3.2 Evaluation of collagen deposition by Picro-Sirius Red staining

Collagen deposition in the scar tissue was stained using Picro-Sirius Red (ESI Table S1 and Fig. S1†). The nucleus was stained blue, while the collagen in the tissue was stained red. The corresponding quantification of the collagen (Fig. 5) revealed that the densities of fibrosis in the control kept the same level through 42 days, but there were significant reductions of fibrosis in the groups of LCP, PC, PU, PLGA, and PMMA during the treatment.

3.3 Expression of α-SMA and Ki-67 in the scar tissues by immunohistochemistry

α-SMA and Ki-67 were two specific marker proteins, expressing in the scar tissues. The nucleus is stained blue, while the target protein is stained brown. α-SMA mainly locates at the cells of the
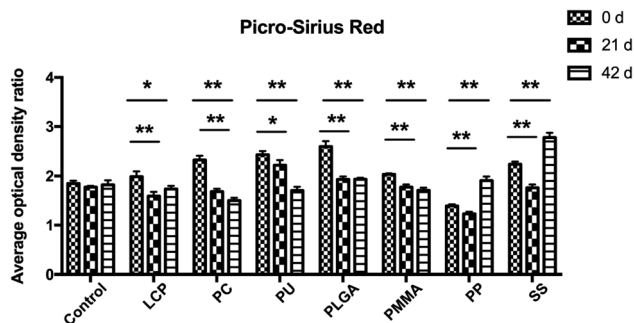

Fig. 5 The average optical density (AOD) ratio of Picro-Sirius Red staining evaluated using software Image J at different time points. LCP, PC, PU, PLGA, PMMA groups show significant reductions of fibrosis during the treatment. *$p < 0.05$ and **$p < 0.001$ vs. 0 days ($n = 3$).
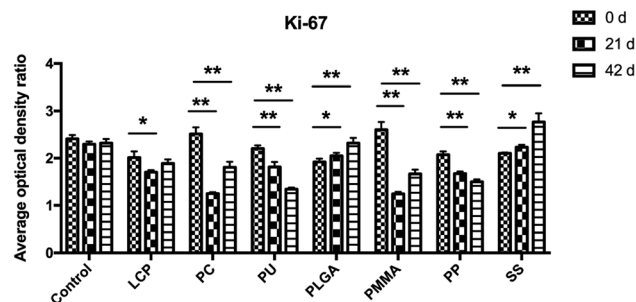

Fig. 7 The average optical density (AOD) ratio of Ki-67 staining evaluated using software Image J at different time points. The treatment using LCP, PC, PU, PMMA, and PP reduced the expression of Ki-67 on day 42. *$p < 0.05$ and **$p < 0.001$ vs. 0 day ($n = 3$).
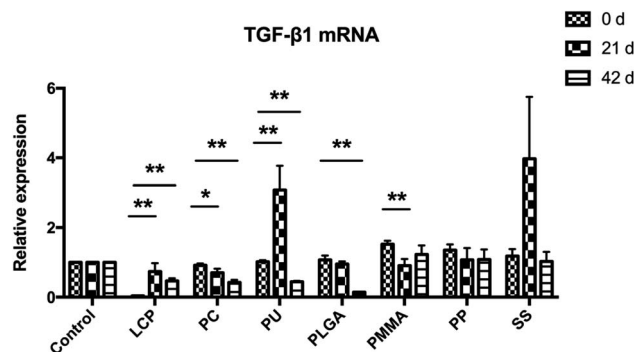
Fig. 8 The expression of TGF-β1 mRNA level in the scar tissue during the MN treatment. The expression of TGF-β1 mRNA was decreased after the treatment of PC, PLGA, PMMA and PP MNs on day 42. $*p < 0.05$ and $**p < 0.001$ *vs.* 0 days ($n = 3$).

dermis, while Ki-67 locates at the epidermal basal layer as well as the dermis.

During these 42 days, the expressions of α-SMA in the scar tissues of the control group increased. However, the α-SMA expression in the groups of PU, PLGA, PMMA, and SS MNs decreased or kept at the same level as day 0 (Fig. 6 and ESI Table S1 and Fig. S2†).

Similarly, we analyzed the expression of Ki-67 protein in the scar tissues (Fig. 7 and ESI Table S1 and Fig. S3†). During these 42 days, the expressions of Ki-67 protein in the control group kept constant. The treatment using LCP, PC, PU, PMMA, and PP reduced the expression of Ki-67.

3.4 The expression of TGF-β1 mRNA in the scar tissue

The expression of TGF-β1 mRNA in the scar tissues was evaluated using qRT-PCR (Fig. 8). While the expression of TGF-β1 mRNA in the control kept constant, it was decreased after the treatment of PC, PLGA, PMMA and PP MNs. Meanwhile, PC and PLGA MN treated groups showed significant decreases compared to other MN treated groups 42 days after the treatment ($P < 0.05$).

4 Discussion

Hypertrophic scars and keloids are benign fibroproliferative skin lesions that commonly occur after trauma or injury as a consequence of an imperfect tissue regeneration. Although several treatment modalities for scars have been put forth, no satisfactory treatment has been identified and multiple side-effects such as significant pain accompany these treatments.[19] Our team has begun to explore the application of MN technology in the treatment of scars since 2012.[13,14] We discovered that drug-free MNs exhibited contact-dependent inhibition on keloids and fibroblast proliferation in the studies performed. This MN device structure consists of an array of needles and a backing surface which is conducive to combine the patch with the skin without affecting the penetration of the skin. These results implied that MNs have the potential to suppress the formation and growth of abnormal scars with few side-effects. The efficacy of LCP dressing MNs in keloids has been

incidentally certified by laboratory experiments and was further proved in clinic trials in keloid patients. Herein, more flexible biopolymers such as poly(ethylene glycol)diacrylate or even clinically compatible materials such as SS need to be fabricated to explore superiority in terms of scar treatment.

This study examined MNs made of LCP, PC, PU, PLGA, PMMA, PP, or SS. The results indicated the thicknesses of scars were significantly decreased in each MN treated group compared to the blank group. However, the decrease of thickness showed no significant difference among MN treated groups. Later we carried four analyses of the scar tissue at the molecular level including collagen deposition, α-SMA and Ki-67 protein expression, and TGF-β1 mRNA expression. The quantification revealed that PMMA is the only one suppressing the expression/deposition of all four biomarkers. Three other polymers (PU, PC, and PLGA) can suppress expression of the three biomarkers: PU decreased collagen, α-SMA and Ki-67 protein expression; PC decreased collagen, Ki-67 protein, and TGF-β1 mRNA; PLGA decreased collagen, α-SMA protein, and TGF-β1 mRNA. Two other polymers (LCP and PP) can only decrease the expression of two biomarkers. As is known, both α-SMA and Ki-67 are highly expressed during the generation of scars. The expression of α-SMA protein is associated with tissue remodeling and scar generation, and is increased in immature scar tissues. The persistent existence of α-SMA protein in hypertrophic scars and keloids implies an abnormal progress to mature normal scars.[20] Ki-67 is a marker of cellular proliferation, and the high expression of Ki-67 in epidermis and dermis indicates continuous progress of scar tissue. And, TGF-β1 mRNA has been investigated with regards to fibrosis-inducing cytokines, which can promote fibroblast differentiation towards myofibroblasts and stimulate collagen and fibronectin synthesis.[17,21] These results suggest that PMMA, PU, PC and PLGA could be better candidates than LCP used in our previous studies.[14]

There are also some improvements to be made in the future study. The long-term safety of MNs was not evaluated and the observation time (up to 42 days) was too short to detect long-term effects. The anti-scar effectiveness index such as vascularization and pigmentation were not analyzed in this study. More study needs to be designed to explore the pliability of MNs on particular scar lesions.

5 Conclusion

MNs showed a remarkable efficacy for scar healing by inhibiting the formation of collagen fibers in the rabbit ear hypertrophic scar models. In comparison to the control group, the treatments of MNs showed different levels of expression for the scar biomarkers including collagen deposition, α-SMA and Ki-67 protein expression, and TGF-β1 mRNA expression. Among these materials, PMMA MNs demonstrated superiority in decreasing the expression level of all four biomarkers while PU, PC, and PLGA could suppress three biomarker expressions. This study reveals that the fabricating materials of MNs should be carefully selected if drug-free MNs are used to treat scars. In future, we will continue to understand the chemical/physical/mechanical mechanism behind this phenomenon.

Data availability

The data and materials are available from the corresponding authors on reasonable request.

Author contributions

MZ, CX and HS conceived the idea, designed the experiments, and wrote the manuscript. HC, SX and DZ performed the experiments. FL and YL collected and analyzed the data and revised the manuscript.

Conflicts of interest

The authors declare no conflicts of interest.

Acknowledgements

References

1 G. C. Limandjaja, F. B. Niessen, R. J. Scheper and S. Gibbs, The Keloid Disorder: Heterogeneity, Histopathology, Mechanisms and Models, *Front. Cell Dev. Biol.*, 2020, **8**, 360.

2 H. Lee and Y. Jang, Recent Understandings of Biology, Prophylaxis and Treatment Strategies for Hypertrophic Scars and Keloids, *Int. J. Mol. Sci.*, 2018, **19**, 711.

3 S. Singh and A. S. Gautam, Upregulated LOX-1 Receptor: Key Player of the Pathogenesis of Atherosclerosis, *Curr. Atheroscler. Rep.*, 2019, **21**, 38.

4 S. Zhang, J. Hou, Q. Yuan, P. Xin, H. Cheng, Z. Gu and J. Wu, Arginine derivatives assist dopamine-hyaluronic acid hybrid hydrogels to have enhanced antioxidant activity for wound healing, *Chem. Eng. J.*, 2020, **392**, 123775.

5 Q. Ou, S. Zhang, C. Fu, L. Yu, P. Xin, Z. Gu, Z. Cao, J. Wu and Y. Wang, More natural more better: triple natural anti-oxidant puerarin/ferulic acid/polydopamine incorporated hydrogel for wound healing, *J. Nanobiotechnol.*, 2021, **19**, 237.

6 P. D. Butler, M. T. Longaker and G. P. Yang, Current progress in keloid research and treatment, *J. Am. Coll. Surg.*, 2008, **206**, 731.

7 S. Monstrey, E. Middelkoop, J. J. Vranckx, F. Bassetto, U. E. Ziegler, S. Meaume and L. Téot, Updated Scar Management Practical Guidelines: Non-invasive and invasive measures, *J. Plast. Reconstr. Aesthet. Surg.*, 2014, **67**, 1017.

8 S. Meaume, A. Le Pillouer-Prost, B. Richert, D. Roseeuw and J. Vadoud, Management of scars: updated practical guidelines and use of silicones, *Eur. J. Dermatol.*, 2014, **24**, 435.

9 A. Nast, S. Eming, J. Fluhr, K. Fritz, G. Gauglitz, S. Hohenleutner, R. G. Panizzon, G. Sebastian, B. Sporbeck and J. Koller, German S2k guidelines for the therapy of pathological scars (hypertrophic scars and keloids), *J. Dtsch. Dermatol. Ges.*, 2012, **10**, 747.

10 O. Kloeters, A. Tandara and T. A. Mustoe, Hypertrophic scar model in the rabbit ear: a reproducible model for studying scar tissue behavior with new observations on silicone gel sheeting for scar reduction, *Wound Repair Regen.*, 2007, **15**, S40.

11 S. Gupta and V. K. Sharma, Standard guidelines of care: Keloids and hypertrophic scars, *Indian J. Dermatol. Venereol. Leprol.*, 2011, **77**, 94.

12 P. Xue, D. C. L. Yeo, Y. J. Chuah, H. L. Tey, Y. Kang and C. Xu, Drug-eluting microneedles for self-administered treatment of keloids, *Technology*, 2014, **2**, 144.

13 D. C. Yeo, E. R. Balmayor, J.-T. Schantz and C. Xu, Microneedle physical contact as a therapeutic for abnormal scars, *Eur. J. Med. Res.*, 2017, **22**, 1.

14 C. Tan, D. Yeo Chen Long, T. Cao, V. Tan Wei Ding, R. Srivastava, A. P. Yow, W. P. Tan, D. Wong Wing Kee, C. Xu and H. L. Tey, Drug-free microneedles in the treatment of keloids: a single-blinded intraindividual controlled clinical trial, *Br. J. Dermatol.*, 2018, **179**, 1418.

15 X. Ning, C. Wiraja, W. T. S. Chew, C. Fan and C. Xu, Transdermal delivery of Chinese herbal medicine extract using dissolvable microneedles for hypertrophic scar treatment, *Acta Pharm. Sin. B*, 2021, **11**, 2937.

16 Y. Yang, L. Xia, X. Ning, T. Hu, C. Xu and W. Liu, Enhanced Drug Permeation into Human Keloid Tissues by Sonophoresis-Assisted Microneedling, *SLAS Technol.*, 2021, **26**, 660.

17 R. C. de Oliveira and S. E. Wilson, Fibrocytes, Wound Healing, and Corneal Fibrosis, *Investig. Ophthalmol. Vis. Sci.*, 2020, **61**, 28.

18 Y. Tai, E. L. Woods, J. Dally, D. Kong, R. Steadman, R. Moseley and A. C. Midgley, Myofibroblasts: Function, Formation, and Scope of Molecular Therapies for Skin Fibrosis, *Biomolecules*, 2021, **11**, 1095.

19 K. Che, Q. Lyu and G. Ma, Comparative Efficacy and Safety of Common Therapies in Keloids and Hypertrophic Scars: A Systematic Review and Meta-analysis, *Aesthetic Plast. Surg.*, 2021, **45**, 372.

20 G. C. Limandjaja, J. M. Belien, R. J. Scheper, F. B. Niessen and S. Gibbs, Hypertrophic and keloid scars fail to progress from the CD34 −/α-smooth muscle actin (α-SMA)+ immature scar phenotype and show gradient differences in α-SMA and p16 expression, *Br. J. Dermatol.*, 2019, **182**, 974.

21 X. Wang, P. Smith, L. L. Pu, Y. J. Kim, F. Ko and M. C. Robson, Exogenous Transforming Growth Factor, *J. Surg. Res.*, 1999, **87**, 194.